ACS Medicinal Chemistry Letters

pubs.acs.org/acsmedchemlett

Letter

Development of Pyrazolo[3,4-*d*]pyrimidine Kinase Inhibitors as Potential Clinical Candidates for Glioblastoma Multiforme

Chiara Greco,[#] Vincenzo Taresco,[#] Amanda K. Pearce, Catherine E. Vasey, Stuart Smith, Ruman Rahman, Cameron Alexander, Robert J. Cavanagh,* Francesca Musumeci,* and Silvia Schenone

Cite This: *ACS Med. Chem. Lett.* 2020, 11, 657−663

Read Online

ACCESS | Metrics & More | Article Recommendations | Supporting Information

ABSTRACT: Glioblastoma multiforme (GBM) is the most aggressive primary brain tumor. Residual cells at the tumor margin are responsible for up to 85% of GBM recurrences after standard treatment. Despite this evidence, the identification of compounds active on this cell population is still an underexplored field. Herein, starting from the knowledge that kinases are implicated in GBM, we evaluated three in-house pyrazolo[3,4-*d*]pyrimidines active as Src, Fyn, and SGK1 kinase inhibitors against patient derived cell lines from either the invasive region or contrast-enhanced core of GBM. We identified our Src inhibitor, SI306, as a promising lead compound for eradicating invasive GBM cells. Furthermore, aiming at the development of a feasible oral treatment for GBM, we performed a formulation study using 2D inkjet printing to generate soluble polymer−drug dispersions. Overall, this study led to the identification of a set of polymer-formulated pyrazolo[3,4-*d*]pyrimidine kinase inhibitors as promising candidates for GBM preclinical efficacy studies.

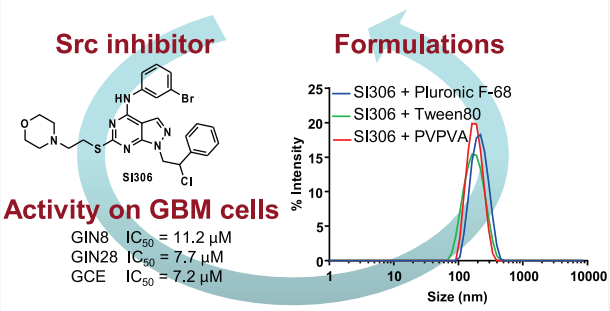

KEYWORDS: *Kinase inhibitors, glioblastoma multiforme, miniaturized assay, inkjet 2D printing, invasive margin cells*

Glioblastoma multiforme (GBM) is the most common, malignant, and aggressive primary brain tumor in adults, mainly due to its rapid proliferation and ability to penetrate and diffusely infiltrate healthy brain parenchyma. Standard of care treatment currently involves a combination of surgery, radiotherapy, and chemotherapy.[1] Yet, despite this multimodal treatment method, the median survival remains poor at less than 15 months.[2] Problems with existing treatment approaches include (i) increased resistance to chemotherapeutic drugs caused by the heterogeneity of the tumor microenvironment and variation in tumor subclones, (ii) inability or impairment of drugs to cross the blood−brain barrier (BBB), and (iii) lack of penetration of locally delivered therapeutic agents deep into the brain parenchyma beyond the resection cavity at sufficient therapeutic concentrations to target residual tumor cells.[3,4] Superior and more innovative treatment methods are necessary to eradicate invasive tumor cells, which remain beyond the resection cavity lining postsurgery, and to block or impair GBM recurrence, which is inevitable with current treatment methods.

The implication of kinases in GBM pathogenesis and drug resistance has led to small molecule kinase inhibitors emerging as possible treatment options.[5,6] Crucially, kinase inhibitors, acting specifically on molecular targets, are purported to reduce off site toxicity during antitumor treatments.[7]

Src-family kinases (SFKs) are a series of nine membrane-associated, nonreceptor tyrosine kinases (c-Src, Fyn, Yes, Lyn, Lck, Blk, Fgr, Hck, and Yrk)[8] that are involved in the regulation of a range of fundamental cellular processes.[9] Previous studies have indicated that dysregulated SFK signaling can induce multiple protumorigenic effects in gliomas, including reduced apoptosis, increased angiogenesis, and increased proliferation.[10−13] Furthermore, evidence suggests that SFKs play roles in cancer cell invasion and metastasis.[14] Src, the most widely studied member of SFKs, is a key downstream intermediate of growth factor receptor pathways and is frequently overexpressed in brain tumors (61% in GBM).[12,15,16] Preclinical data confirmed the key role of Src in GBM proliferation and invasion,[17] leading the way for the use of Src inhibitors in clinical studies. Additionally, Fyn has also been reported to be an effector of oncogenic signaling in GBM patients.[18]

In 2009, Lu et al. identified that persistent epidermal growth factor receptor (EGFR) signaling activated both Fyn and Src

Special Issue: In Memory of Maurizio Botta: His Vision of Medicinal Chemistry

Received: November 18, 2019
Accepted: February 13, 2020
Published: February 13, 2020

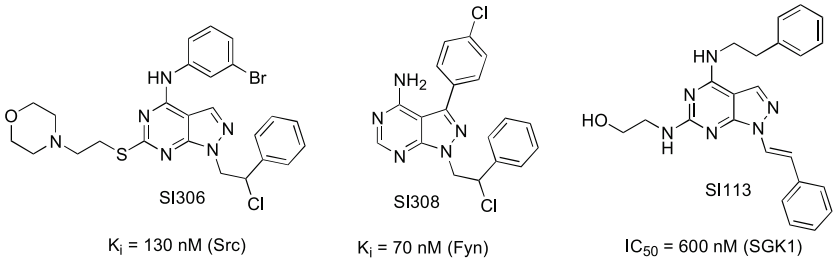

Figure 1. Structures of in-house kinase inhibitors SI306, SI308, and SI113 and their activity toward Src, Fyn, and SGK1.

to increase GBM invasion and tumor survival *in vivo*.[18] More recently, Comba et al. demonstrated the correlation of Fyn expression with malignant features of GBM tumors, including pseudopalisades, necrosis, and hypervascularization.[19]

Dasatinib, a broad spectrum inhibitor of SFKs, including Src, Fyn and Lyn, has been proposed as a therapeutic option in recurrent GBM.[14] Dasatinib was well tolerated in clinical trials but failed to improve overall survival either as a monotherapy or in combination therapy for GBM patients,[20,21] a result attributed to its susceptibility to cellular efflux by transporters and subsequent poor accumulation in brain tissue.[22] Generally, no kinase inhibitor trial (e.g., EGFR and PDGFR) has had phase II survival benefit for GBM patients.[23,24]

In addition to SFKs, other kinases have been investigated for their role in GBM pathogenesis, including serum- and glucocorticoid-regulated kinase 1 (SGK1) which has been associated with neoplastic transformation, and chemo/radioresistance.[25,26]

Over recent years, our group has designed and synthesized a wide library of pyrazolo[3,4-*d*]pyrimidines active as kinase inhibitors.[27,28] In particular, three of our in-house compounds (SI306, SI308, and SI113 (Figure 1)) have been shown to be potent inhibitors of the tyrosine kinases Src and Fyn and serine-threonine kinase SGK1,[29−31] respectively, and have demonstrated anticancer effects on different commercial (established) GBM cell lines.[30,32,33]

However, most commercial GBM cell lines have historically been derived from the core region of tumors, which does not allow a realistic, phenotypically accurate representation of the infiltrative cells which ultimately result in the inevitable recurrence of GBM.[3] Significantly, residual cells at the tumor margin are responsible for the 85% of GBMs that relapse locally after maximal safe surgical resection followed by the standard combination protocol of temozolomide and radiotherapy.[34] Therefore, the discovery of molecules active against invasive GBM cells represents a crucial step in the development of drugs for the treatment of this pathology.[35]

We evaluated the cytotoxicity of kinase inhibitors on primary patient derived cell lines from the invasive region (GIN8, GIN28) and on the corresponding central tumor core (GCE28) cell line from the same patient, and we assessed the anticancer effects of our kinase inhibitors in monotherapy and combination therapy. Furthermore, since our compounds can be considered in biopharmaceutical classification system (BCS) class II,[36] demonstrating good permeability[37] (indicating a good probability of BBB permeation, which is further supported by previous work on our compounds[38]) but limited water solubility, we performed a formulation study, applying the innovative inkjet printing technology to generate solid dispersions of our lead compound inhibitor in inert hydrophilic polymeric carriers. This formulation strategy, recently reported by us,[39] can be used to increase the water solubility of the inhibitors in a manner that does not compromise potency and thus provides a viable approach for development of oral formulations.

In vitro data demonstrated that the different kinase inhibitors were cytotoxic, implicating Src, Fyn, and SGK1 kinases as valid targets in the tested GBM cell lines. SI306 (Src inhibitor) was demonstrated to be the most potent tested compound with IC_{50} values of 11.2, 7.7, and 7.2 μM in the GIN8, GIN28, and GCE28 cell lines, respectively. Compound SI113 (SGK1 inhibitor) exhibited similar potency to SI306 in the GIN8 line but was 1.9-fold and 1.5-fold less potent in GIN28 and GCE28 cells. The least potent compound was shown to be SI308 (Fyn inhibitor), with IC_{50} values 4.9-fold, 6.5-fold, and 6.6-fold higher than the most potent compound (SI306), in GIN8, GIN28, and GCE28 cells, respectively (Table 1 and Figure 4SI). However, despite being the least potent compound in monotherapy, SI308 demonstrated a promising application in synergistic combination therapy with a Scr inhibitor, as described later.

Table 1. IC_{50} Values of Kinase Inhibitors on GBM Cells[a]

	IC_{50} (μM)		
compd	GIN8	GIN28	GCE28
SI306	11.2 ± 3.8	7.7 ± 1.6	7.2 ± 2.0
SI308	54.7 ± 6.3	49.8 ± 4.2	47.6 ± 6.9
SI113	10.5 ± 3.5	14.4 ± 2.8	10.7 ± 1.2

[a]Potency was assessed with PrestoBlue assay. Compounds were applied diluted in 10% FBS containing DMEM for 48 h. Data represent the mean ± SE. IC_{50} values were calculated from three independent experiments. Statistical significance was determined via two-way ANOVA followed by Dunnett's multiple comparisons test.

Following the confirmation of compound cytotoxicity, we next investigated the effector caspases-3/7 to determine if cell death was apoptotic in nature.[40]

Data in Figure 2 demonstrate that at a cytotoxic concentration (12.5 μM), SI113 and SI306 induce significant increases in caspase-3/7 activation in all GBM cell lines tested with the exception of SI113 in the GIN28 line.

For assay verification, staurosporine (10.0 μM), a known inducer of apoptosis,[41] was also tested as a reference compound. It elicits significant increase in caspase activation at similar or lower levels than those of the kinase inhibitors. It can be noted that SI306 induces higher levels of effector caspase activation compared to SI113, a result that reflects the IC_{50} data (Table 1) which together indicate that SI306 is the most active compound we tested against these cell lines.

To further confirm the apoptotic death induced by SI306, the nuclear morphology and permeability were investigated by

https://dx.doi.org/10.1021/acsmedchemlett.9b00530
ACS Med. Chem. Lett. 2020, 11, 657−663

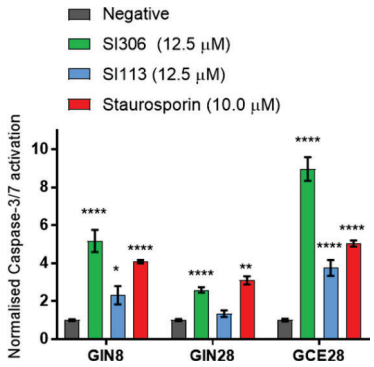

Figure 2. Effect of kinase inhibitors on levels of activated effector caspases-3/7 on GBM cells. Compounds were applied diluted in 10% FBS containing DMEM for 48 h. Caspase levels were assessed with the CellEvent caspase-3/7 probe. Data represent the mean ± SEM (n = 3). Statistical significance was determined via two-way ANOVA followed by Dunnett's multiple comparisons test.

fluorescence microscopy using Hoechst 33342 (Ho) and propidium iodide (PI) double staining (Figure 3). Cells treated with SI306 exhibit signs of chromatid condensation, nuclear fragmentation, and the presence of apoptotic bodies, which are well-known proapoptotic features. SI306 treatment did not induce nuclear membrane permeability, as shown by PI negative staining, or nuclear swelling, indicators of necrotic cell death and demonstrated by ethanol (EtOH) (Figure 3), a known inducer of necrosis.[42] These observations, taken together with the effective caspase activation, indicate that SI306 is inducing GBM cell death via an apoptotic mechanism.

Previous evidence indicates that targeting more than one kinase may be beneficial in cancer treatment, creating the opportunity to achieve a synergistic effect and to overcome the development of resistance.[43,44] Therefore, we have investigated our novel compounds as combination therapies in order to assess if synergistic activity can be achieved. The median-effect algorithm based on the widely used method established by Chou and Talalay[45] was employed to calculate the combination index (CI) as outlined in the Supporting Information. The CI equation was used to generate CI values, which categorize the compound−compound combinations as synergistic, additive, or antagonistic. Interestingly, the combination of SI308 with either SI306 or SI113 was determined to generate synergistic effects despite SI308 having been demonstrated to be the least potent compound in monotherapy (Figure 4).

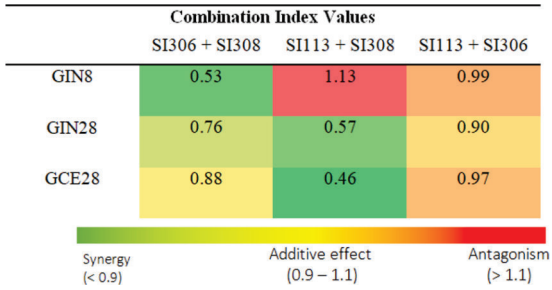

Figure 4. Combination index values. Compounds were applied at a molar ratio of 1:1. Shown is a summary of the CI values for the combinations of kinase inhibitors following 48 h incubation in three GBM lines. Each CI value was calculated, and a heat map was generated on the basis of three independent IC_{50} experiments (n = 3). Values represent the mean ± SD.

On the contrary, SI113 and SI306 co-therapy exhibited only additive action. Therefore, the observed effects suggest that co-inhibition of the Fyn kinase and SGK1 or Src kinases provides a synergistic action that cannot be achieved via inhibiting SGK1 and Src together. Of further note is the observation that in the GIN8 line, co-therapy with SI113 and SI308 produced an antagonistic effect despite synergy being observed in the GIN28 and GCE28 lines with this combination. The reasons for this remain unclear; however, patient genetic variation may play a role (GIN28 and GCE28 lines are derived from the same patient, and the GIN8 line is from a separate patient).

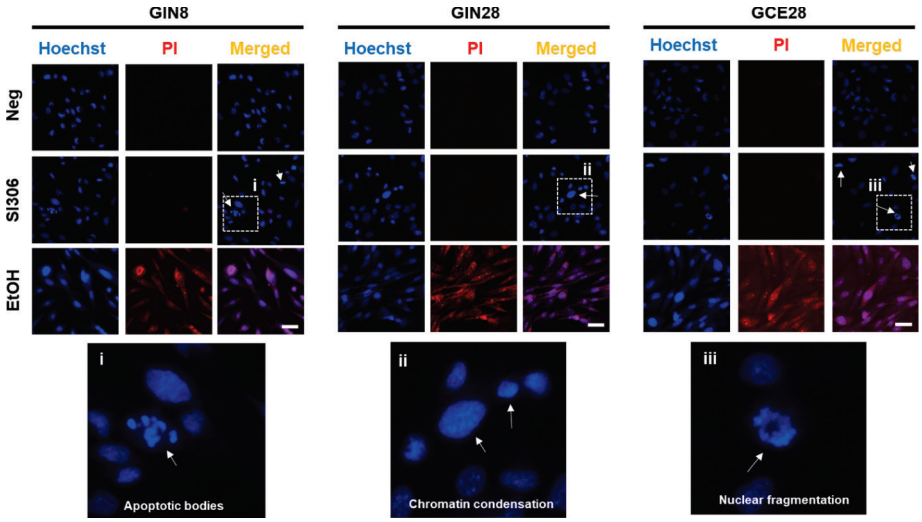

Figure 3. Ho/PI staining of nuclei. Effect of SI306 kinase inhibitor on apoptotic features of cellular nuclei. Cells were dosed with 12.5 μM SI306, 70% ethanol (EtOH) or DMEM (Neg, negative control) for 48 h followed by nuclear staining with Hoechst 33342 and propidium iodide dyes. Scale bar indicates 30 μm. Images shown are representative of three sets of independent images. White arrows indicate the presence of apoptotic nuclei (chromatid condensation, apoptotic bodies).

https://dx.doi.org/10.1021/acsmedchemlett.9b00530
ACS Med. Chem. Lett. 2020, 11, 657−663

Taken together, the evidence for synergistic action with our compounds may promote the adoption of combination therapies in the field of kinase inhibitors[46] for the treatment of resistant GBM.

The promising *in vitro* data highlight pyrazolo[3,4-*d*]-pyrimidine kinase inhibitors as potential pharmacotherapies for eradicating invasive GBM cell lines. To further their development for clinical application, we have investigated the formulation of our lead compound SI306. To overcome the water solubility limitation of SI306, which may affect further *in vivo* studies and future oral administration routes, we performed a preliminary formulation screening process based on 2D inkjet printing, building on an approach previously validated by our group.[39,47,48] Different commercial polymers were combined with SI306 and the apparent-solubility (ΔA%) value of each formulation was calculated in order to identify the polymers able to solubilize our lead compound (Figure 5).

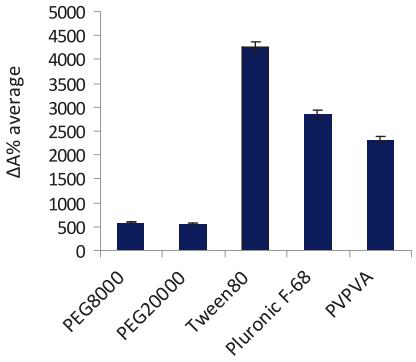

Figure 5. ΔA% average of SI306-polymer formulation ranked according to their water apparent-solubility enhancement (high ΔA % is related to a high compound water solubility). Data represent the mean ± SEM (n = 3).

Data demonstrate that two surfactants (Pluronic F-68 and Tween 80) and the amphiphilic copolymer PVPVA showed notably higher ΔA% average values compared to the highly hydrophilic homopolymers (PEG8000−20000) (see Supporting Information, Table 1SI and Figures 1SI and 2SI for further details).

These results suggest that solubilization of hydrophobic SI306 is due to associative interactions between hydrophobic blocks in Pluronic F-68, Tween 80, and PVPVA and the lipophilic regions in SI306.[39] Dynamic light scattering (DLS) measurements were performed on the formulation of SI306 with the three candidate polymers Pluronic F-68, Tween 80, and PVPVA (Figure 6) in order to evaluate the particulate nature of the drug−polymer assemblies.

As can be observed from Figure 6, all the formulations produced well-defined nanoaggregates, characterized by a single monomodal and monodispersed population with sizes ranging from 180 to 200 nm, confirming the quality of the nanoformulations.

To further validate the water solubility enhancement, we performed a cytotoxicity assay using SI306 either dissolved in DMSO or printed into the selected polymers. Negative control, polymers alone, and SI306 suspended in PBS and diluted in cell culture medium DMEM (to highlight SI306 poor water solubility and consequent *in vitro* inactivity) had no effect on cell viability. On the contrary, formulated SI306

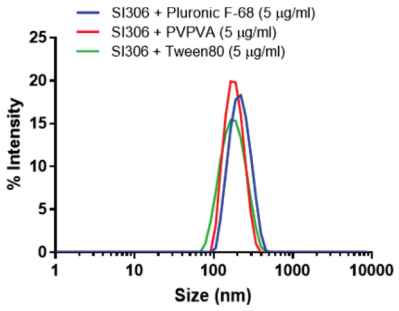

Figure 6. DLS traces in PBS of SI306 as a formulation. Light scattering measurements were collected on suspensions prepared with a final concentration of 5 μg/mL.

resuspended in DMEM and SI306 dissolved in DMSO treatments had comparable cytotoxic effects on all GBM cell lines (Figure 7).

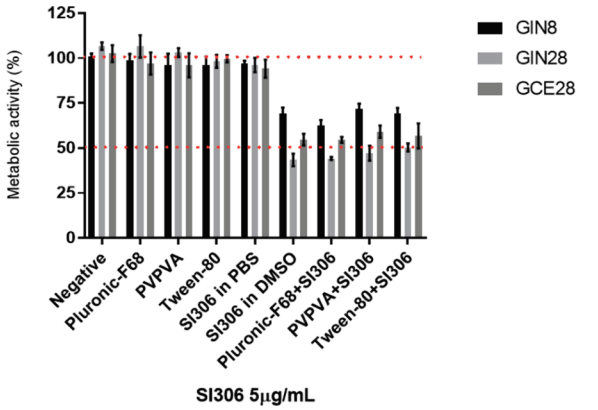

Figure 7. Compound SI306 formulated with the selected best polymers was then tested against the patients derived GBM cell lines and the potency compared to the compound solubilized in 1% DMSO. Potency was assessed after 48 h with PrestoBlue assay. Data represent the mean ± SD.

Therefore, the described SI306 formulation can successfully increase the apparent water solubility of the inhibitor without affecting its potency, and this provides a further step into the development of our lead compound.

It is noteworthy that no kinase inhibitor has yet shown clinical benefit in GBM. The reasons for this are complex and multifactorial and include failure to achieve BBB penetration, genetic heterogeneity in the tumor, target redundancy, and rapid molecular adaptation. On the other hand, kinase inhibitors have certainly shown benefit in other aggressive forms of cancer such as non-small-cell lung cancer[49] and renal cancer,[50] and for these reasons, they can be considered promising drugs for GBM therapy if the above problems are overcome (Figure 8). Pyrazolo[3,4-*d*]pyrimidines synthesized by our group were able to cross the BBB,[38,51] laying the foundation for a successful development.

In conclusion, we have evaluated the potency of our pyrazolo[3,4-*d*]pyrimidines active as specific kinase inhibitors, against patient derived cell lines from the invasive region and core of GBM, identifying the Src inhibitor SI306 as a lead compound. SI306 possesses an IC_{50} in the low micromolar range on all the three GBM cell lines tested in this work,

https://dx.doi.org/10.1021/acsmedchemlett.9b00530
ACS Med. Chem. Lett. 2020, 11, 657−663

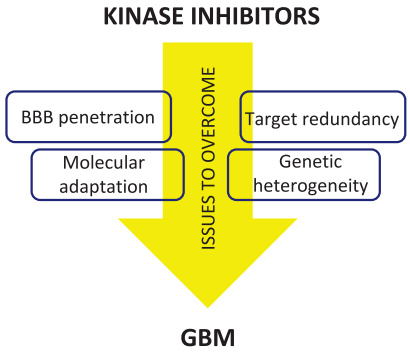

Figure 8. Simplified representation of the main issues that kinase inhibitors have to overcome to obtain clinical benefits in GBM therapy.

demonstrating the ability to induce apoptotic death. A combination study, using the Chou and Talalay method, has also been assessed and showed that, based on patient genetic variations, our kinase inhibitors possess a synergistic effect that could positively influence the success of GBM treatment.

Lastly, a polymer formulation strategy involving the novel 2D inkjet printing technology was explored as a strategy to enhance SI306 water solubility. *In vitro* results illustrated that printing 5 μg/mL of our lead compound into dispersions of Pluronic F-68, Tween 80, or PVPVA at a level of 90% is a successful formulation method, resulting in a comparable potency to SI306 dissolved in DMSO. Accordingly, this methodology provides a viable approach for the development of oral formulations of our in-house kinase inhibitors. Furthermore, since some of the chosen polymers, such as the Pluronic family, have been shown to facilitate transport across the BBB, a next challenge could be the selection of the best polymer for *in vivo* GBM studies.

Overall, these results encourage *in vivo* studies and promote polymer-carried pyrazolo[3,4-*d*]pyrimidine kinase inhibitors as oral feasible treatments against GBM potentially active also against tumor recurrence.

■ ASSOCIATED CONTENT

Supporting Information

The Supporting Information is available free of charge at https://pubs.acs.org/doi/10.1021/acsmedchemlett.9b00530.

General information on chemicals, experimental details for the printing, UV screening, DLS, and cellular assays (PDF)

■ AUTHOR INFORMATION

Corresponding Authors

Robert J. Cavanagh − *School of Pharmacy, University of Nottingham, Nottingham NG7 2RD, U.K.*; Email: Robert.Cavanagh1@nottingham.ac.uk

Francesca Musumeci − *Department of Pharmacy, University of Genoa, 16132 Genoa, Italy*; orcid.org/0000-0002-7228-0086; Email: francesca.musumeci@unige.it

Authors

Chiara Greco − *Department of Pharmacy, University of Genoa, 16132 Genoa, Italy*

Vincenzo Taresco − *School of Chemistry, University of Nottingham, Nottingham NG7 2RD, U.K.*; orcid.org/0000-0003-4476-8233

Amanda K. Pearce − *School of Chemistry, University of Birmingham, Birmingham B15 2TT, U.K.*; orcid.org/0000-0003-3372-7380

Catherine E. Vasey − *School of Pharmacy, University of Nottingham, Nottingham NG7 2RD, U.K.*

Stuart Smith − *Children's Brain Tumour Research Centre, School of Medicine, University of Nottingham, Nottingham NG7 2UH, U.K.*

Ruman Rahman − *Children's Brain Tumour Research Centre, School of Medicine, University of Nottingham, Nottingham NG7 2UH, U.K.*

Cameron Alexander − *School of Pharmacy, University of Nottingham, Nottingham NG7 2RD, U.K.*; orcid.org/0000-0001-8337-1875

Silvia Schenone − *Department of Pharmacy, University of Genoa, 16132 Genoa, Italy*

Complete contact information is available at: https://pubs.acs.org/10.1021/acsmedchemlett.9b00530

Author Contributions

#C.G. and V.T. contributed equally. The manuscript was written through contributions of all authors. All authors have given approval to the final version of the manuscript.

Funding

This work was supported by the Italian MIUR Project PRIN 2017 2017SA5837_004 (S.S. and F.M.) and the Engineering and Physical Sciences Research Council [Grants EP/N006615/1, EP/N03371X/1, EP/L01646X/1, EP/H005625/1, EP/L013835/1, and EP/R035563/1] (C.A.). This work was also funded by the Royal Society [Wolfson Research Merit Award WM150086] to C.A.

Notes

The authors declare no competing financial interest.

■ ABBREVIATIONS

BBB, blood−brain barrier; BCS, biopharmaceutical classification system; CI, combination index; DLS, dynamic light scattering; DMEM, Dulbecco's modified Eagle medium; DMSO, dimethyl sulfoxide; GBM, glioblastoma multiforme; Ho, Hoechst 33342; PBS, phosphate buffered saline; PEG, polyethylene glycol; PI, propidium iodide; PVPVA, polyvinylpyrrolidone-vinyl acetate; SFK, Src-family kinase; SGK1, serum- and glucocorticoid-regulated kinase 1

■ REFERENCES

(1) Batash, R.; Asna, N.; Schaffer, P.; Francis, N.; Schaffer, M. Glioblastoma multiforme, diagnosis and treatment; recent literature review. *Curr. Med. Chem.* **2017**, *24* (27), 3002−3009.

(2) Alifieris, C.; Trafalis, D. T. Glioblastoma multiforme: pathogenesis and treatment. *Pharmacol. Ther.* **2015**, *152*, 63−82.

(3) Perrin, S. L.; Samuel, M. S.; Koszyca, B.; Brown, M. P.; Ebert, L. M.; Oksdath, M.; Gomez, G. A. Glioblastoma heterogeneity and the tumour microenvironment: implications for preclinical research and development of new treatments. *Biochem. Soc. Trans.* **2019**, *47* (2), 625−638.

(4) Lemée, J.-M.; Clavreul, A.; Menei, P. Intratumoral heterogeneity in glioblastoma: don't forget the peritumoral brain zone. *Neuro. Oncol.* **2015**, *17* (10), 1322−1332.

(5) Carrasco-García, E.; Saceda, M.; Martínez-Lacaci, I. Role of receptor tyrosine kinases and their ligands in glioblastoma. *Cells* **2014**, *3* (2), 199−235.

(6) Li, X.; Wu, C.; Chen, N.; Gu, H.; Yen, A.; Cao, L.; Wang, E.; Wang, L. PI3K/Akt/MTOR signaling pathway and targeted therapy for glioblastoma. *Oncotarget* **2016**, *7* (22), 33440−33450.

(7) Arora, A.; Scholar, E. M. Role of Tyrosine kinase inhibitors in cancer therapy. *J. Pharmacol. Exp. Ther.* **2005**, *315* (3), 971−979.
(8) Yeatman, T. J. A Renaissance for SRC. *Nat. Rev. Cancer* **2004**, *4* (6), 470−480.
(9) Roskoski, R. Src protein-tyrosine kinase structure, mechanism, and small molecule inhibitors. *Pharmacol. Res.* **2015**, *94*, 9−25.
(10) Lewis-Tuffin, L. J.; Feathers, R.; Hari, P.; Durand, N.; Li, Z.; Rodriguez, F. J.; Bakken, K.; Carlson, B.; Schroeder, M.; Sarkaria, J. N.; Anastasiadis, P. Z. Src Family kinases differentially influence glioma growth and motility. *Mol. Oncol.* **2015**, *9* (9), 1783−1798.
(11) Park, C.-M.; Park, M.-J.; Kwak, H.-J.; Lee, H.-C.; Kim, M.-S.; Lee, S.-H.; Park, I.-C.; Rhee, C. H.; Hong, S.-I. Ionizing radiation enhances matrix metalloproteinase-2 secretion and invasion of glioma cells through src/epidermal growth factor receptor-mediated P38/Akt and phosphatidylinositol 3-Kinase/Akt signaling pathways. *Cancer Res.* **2006**, *66* (17), 8511−8519.
(12) Eskilsson, E.; Rosland, G. V.; Talasila, K. M.; Knappskog, S.; Keunen, O.; Sottoriva, A.; Foerster, S.; Solecki, G.; Taxt, T.; Jirik, R.; Fritah, S.; Harter, P. N.; Välk, K.; Al Hossain, J.; Joseph, J. V.; Jahedi, R.; Saed, H. S.; Piccirillo, S. G.; Spiteri, I.; Leiss, L.; Euskirchen, P.; Graziani, G.; Daubon, T.; Lund-Johansen, M.; Enger, P.Ø.; Winkler, F.; Ritter, C. A.; Niclou, S. P.; Watts, C.; Bjerkvig, R.; Miletic, H. EGFRvIII mutations can emerge as late and heterogenous events in glioblastoma development and promote angiogenesis through Src activation. *Neuro Oncol* **2016**, *18* (12), 1644−1655.
(13) Liu, W. M.; Huang, P.; Kar, N.; Burgett, M.; Muller-Greven, G.; Nowacki, A. S.; Distelhorst, C. W.; Lathia, J. D.; Rich, J. N.; Kappes, J. C.; Gladson, C. L. Lyn facilitates glioblastoma cell survival under conditions of nutrient deprivation by promoting autophagy. *PLoS One* **2013**, *8* (8), No. e70804.
(14) Huveldt, D.; Lewis-Tuffin, L. J.; Carlson, B. L.; Schroeder, M. A.; Rodriguez, F.; Giannini, C.; Galanis, E.; Sarkaria, J. N.; Anastasiadis, P. Z. Targeting Src family kinases inhibits Bevacizumab-induced glioma cell invasion. *PLoS One* **2013**, *8* (2), No. e56505.
(15) Du, J.; Bernasconi, P.; Clauser, K. R.; Mani, D. R.; Finn, S. P.; Beroukhim, R.; Burns, M.; Julian, B.; Peng, X. P.; Hieronymus, H.; Maglathlin, R. L.; Lewis, T. A.; Liau, L. M.; Nghiemphu, P.; Mellinghoff, I. K.; Louis, D. N.; Loda, M.; Carr, S. A.; Kung, A. L.; Golub, T. R. Bead-based profiling of tyrosine kinase phosphorylation identifies SRC as a potential target for glioblastoma therapy. *Nat. Biotechnol.* **2009**, *27* (1), 77−83.
(16) Yamaguchi, K.; Kugimiya, T.; Miyazaki, T. Substance P receptor in U373 MG human astrocytoma cells activates mitogen-activated protein kinases ERK1/2 through Src. *Brain Tumor Pathol.* **2005**, *22* (1), 1−8.
(17) Ahluwalia, M. S.; de Groot, J.; Liu, W. M.; Gladson, C. L. Targeting SRC in glioblastoma tumors and brain metastases: rationale and preclinical studies. *Cancer Lett.* **2010**, *298* (2), 139−149.
(18) Lu, K. V.; Zhu, S.; Cvrljevic, A.; Huang, T. T.; Sarkaria, S.; Ahkavan, D.; Dang, J.; Dinca, E. B.; Plaisier, S. B.; Oderberg, I.; Lee, Y.; Chen, Z.; Caldwell, J. S.; Xie, Y.; Loo, J. A.; Seligson, D.; Chakravari, A.; Lee, F. Y.; Weinmann, R.; Cloughesy, T. F.; Nelson, S. F.; Bergers, G.; Graeber, T.; Furnari, F. B.; James, C. D.; Cavenee, W. K.; Johns, T. G.; Mischel, P. S. Fyn and SRC are effectors of oncogenic epidermal growth factor receptor signaling in glioblastoma patients. *Cancer Res.* **2009**, *69* (17), 6889−6898.
(19) Comba, A.; Kadiyala, P.; Argento, A. E.; Patel, P.; Nunez, F. J.; Saxena, M.; Castro, M. G.; Lowenstein, P. R. CSIG-39. Fyn, an oncogene that reduces glioblastoma survival yet sensitizes to chemo-radiotherapy. *Neuro. Oncol.* **2017**, *19* (Suppl. 6), vi58−vi58.
(20) Lassman, A. B.; Pugh, S. L.; Gilbert, M. R.; Aldape, K. D.; Geinoz, S.; Beumer, J. H.; Christner, S. M.; Komaki, R.; DeAngelis, L. M.; Gaur, R.; Youssef, E.; Wagner, H.; Won, M.; Mehta, M. P. Phase 2 trial of Dasatinib in target-selected patients with recurrent glioblastoma (RTOG 0627). *Neuro. Oncol.* **2015**, *17* (7), 992−998.
(21) Galanis, E.; Anderson, S. K.; Twohy, E. L.; Carrero, X. W.; Dixon, J. G.; Tran, D. D.; Jeyapalan, S. A.; Anderson, D. M.; Kaufmann, T. J.; Feathers, R. W.; Giannini, C.; Buckner, J. C.; Anastasiadis, P. Z.; Schiff, D. A Phase 1 and randomized, placebo-controlled Phase 2 trial of Bevacizumab plus Dasatinib in patients with recurrent glioblastoma: Alliance/North Central Cancer Treatment Group N0872. *Cancer* **2019**, *125* (21), 3790−3800.
(22) Agarwal, S.; Mittapalli, R. K.; Zellmer, D. M.; Gallardo, J. L.; Donelson, R.; Seiler, C.; Decker, S. A.; SantaCruz, K. S.; Pokorny, J. L.; Sarkaria, J. N.; Elmquist, W. F.; Ohlfest, J. R. Active efflux of Dasatinib from the brain limits efficacy against murine glioblastoma: broad implications for the clinical use of molecularly targeted agents. *Mol. Cancer Ther.* **2012**, *11* (10), 2183−2192.
(23) Taylor, J. W.; Parikh, M.; Phillips, J. J.; James, C. D.; Molinaro, A. M.; Butowski, N. A.; Clarke, J. L.; Oberheim-Bush, N. A.; Chang, S. M.; Berger, M. S.; Prados, M. Phase-2 Trial of Palbociclib in adult patients with recurrent RB1-positive glioblastoma. *J. Neuro-Oncol.* **2018**, *140* (2), 477−483.
(24) Peereboom, D. M.; Ahluwalia, M. S.; Ye, X.; Supko, J. G.; Hilderbrand, S. L.; Phuphanich, S.; Nabors, L. B.; Rosenfeld, M. R.; Mikkelsen, T.; Grossman, S. A. NABTT 0502: A Phase II and pharmacokinetic study of erlotinib and sorafenib for patients with progressive or recurrent glioblastoma multiforme. *Neuro. Oncol.* **2013**, *15* (4), 490−496.
(25) Talarico, C.; Dattilo, V.; D'Antona, L.; Menniti, M.; Bianco, C.; Ortuso, F.; Alcaro, S.; Schenone, S.; Perrotti, N.; Amato, R. SGK1, the new player in the game of resistance: chemo-radio molecular target and strategy for inhibition. *Cell. Physiol. Biochem.* **2016**, *39* (5), 1863−1876.
(26) Kulkarni, S.; Goel-Bhattacharya, S.; Sengupta, S.; Cochran, B. H. A large-scale RNAi screen identifies SGK1 as a key survival kinase for GBM stem cells. *Mol. Cancer Res.* **2018**, *16* (1), 103−114.
(27) Molinari, A.; Fallacara, A. L.; Di Maria, S.; Zamperini, C.; Poggialini, F.; Musumeci, F.; Schenone, S.; Angelucci, A.; Colapietro, A.; Crespan, E.; Kissova, M.; Maga, G.; Botta, M. Efficient optimization of pyrazolo[3,4-*d*]pyrimidines derivatives as c-Src kinase inhibitors in neuroblastoma treatment. *Bioorg. Med. Chem. Lett.* **2018**, *28* (21), 3454−3457.
(28) Radi, M.; Tintori, C.; Musumeci, F.; Brullo, C.; Zamperini, C.; Dreassi, E.; Fallacara, A. L.; Vignaroli, G.; Crespan, E.; Zanoli, S.; Laurenzana, I.; Filippi, I.; Maga, G.; Schenone, S.; Angelucci, A.; Botta, M. Design, Synthesis, and biological evaluation of pyrazolo[3,4-*d*]pyrimidines active in vivo on the Bcr-Abl T315I mutant. *J. Med. Chem.* **2013**, *56* (13), 5382−5394.
(29) Tintori, C.; Fallacara, A. L.; Radi, M.; Zamperini, C.; Dreassi, E.; Crespan, E.; Maga, G.; Schenone, S.; Musumeci, F.; Brullo, C.; Richters, A.; Gasparrini, F.; Angelucci, A.; Festuccia, C.; Delle Monache, S.; Rauh, D.; Botta, M. Combining X-ray crystallography and molecular modeling toward the optimization of pyrazolo[3,4-*d*]pyrimidines as potent c-Src inhibitors active in vivo against neuroblastoma. *J. Med. Chem.* **2015**, *58* (1), 347−361.
(30) Tintori, C.; La Sala, G.; Vignaroli, G.; Botta, L.; Fallacara, A. L.; Falchi, F.; Radi, M.; Zamperini, C.; Dreassi, E.; Dello Iacono, L.; Orioli, D.; Biamonti, G.; Garbelli, M.; Lossani, A.; Gasparrini, F.; Tuccinardi, T.; Laurenzana, I.; Angelucci, A.; Maga, G.; Schenone, S.; Brullo, C.; Musumeci, F.; Desogus, A.; Crespan, E.; Botta, M. Studies on the ATP binding site of Fyn kinase for the identification of new inhibitors and their evaluation as potential agents against tauopathies and tumors. *J. Med. Chem.* **2015**, *58* (11), 4590−4609.
(31) Ortuso, F.; Amato, R.; Artese, A.; D'antona, L.; Costa, G.; Talarico, C.; Gigliotti, F.; Bianco, C.; Trapasso, F.; Schenone, S.; Musumeci, F.; Botta, L.; Perrotti, N.; Alcaro, S. In silico identification and biological evaluation of novel selective Serum/Glucocorticoid-Inducible kinase 1 inhibitors based on the pyrazolo-pyrimidine scaffold. *J. Chem. Inf. Model.* **2014**, *54* (7), 1828−1832.
(32) Calgani, A.; Vignaroli, G.; Zamperini, C.; Coniglio, F.; Festuccia, C.; Di Cesare, E.; Gravina, G. L.; Mattei, C.; Vitale, F.; Schenone, S.; Botta, M.; Angelucci, A. Suppression of SRC signaling is effective in reducing synergy between glioblastoma and stromal cells. *Mol. Cancer Ther.* **2016**, *15* (7), 1535−1544.
(33) Matteoni, S.; Abbruzzese, C.; Matarrese, P.; De Luca, G.; Mileo, A. M.; Miccadei, S.; Schenone, S.; Musumeci, F.; Haas, T. L.; Sette, G.; Carapella, C. M.; Amato, R.; Perrotti, N.; Signore, M.;

https://dx.doi.org/10.1021/acsmedchemlett.9b00530
ACS Med. Chem. Lett. 2020, 11, 657−663

Paggi, M. G. The kinase inhibitor SI113 induces autophagy and synergizes with quinacrine in hindering the growth of human glioblastoma multiforme cells. *J. Exp. Clin. Cancer Res.* **2019**, *38* (1), 202.
(34) Petrecca, K.; Guiot, M.-C.; Panet-Raymond, V.; Souhami, L. Failure pattern following complete resection plus radiotherapy and Temozolomide is at the resection margin in patients with glioblastoma. *J. Neuro-Oncol.* **2013**, *111* (1), 19−23.
(35) Smith, S. J.; Diksin, M.; Chhaya, S.; Sairam, S.; Estevez-Cebrero, M. A.; Rahman, R. The invasive region of glioblastoma defined by 5ALA guided surgery has an altered cancer stem cell marker profile compared to central tumour. *Int. J. Mol. Sci.* **2017**, *18* (11), 2452.
(36) The Biopharmaceutics Classification System (BCS) Guidance.| FDA. https://www.fda.gov/about-fda/center-drug-evaluation-and-research-cder/biopharmaceutics-classification-system-bcs-guidance (accessed Oct 13, 2019).
(37) Radi, M.; Dreassi, E.; Brullo, C.; Crespan, E.; Tintori, C.; Bernardo, V.; Valoti, M.; Zamperini, C.; Daigl, H.; Musumeci, F.; Carraro, F.; Naldini, A.; Filippi, I.; Maga, G.; Schenone, S.; Botta, M. Design, synthesis, biological activity, and ADME properties of pyrazolo[3,4-*d*]pyrimidines active in hypoxic human leukemia cells: a lead optimization study. *J. Med. Chem.* **2011**, *54* (8), 2610−2626.
(38) Ceccherini, E.; Indovina, P.; Zamperini, C.; Dreassi, E.; Casini, N.; Cutaia, O.; Forte, I. M.; Pentimalli, F.; Esposito, L.; Polito, M. S.; Schenone, S.; Botta, M.; Giordano, A. SRC family kinase inhibition through a new pyrazolo[3,4-d]pyrimidine derivative as a feasible approach for glioblastoma treatment. *J. Cell. Biochem.* **2015**, *116* (5), 856−863.
(39) Sanna, M.; Sicilia, G.; Alazzo, A.; Singh, N.; Musumeci, F.; Schenone, S.; Spriggs, K. A.; Burley, J. C.; Garnett, M. C.; Taresco, V.; Alexander, C. Water solubility enhancement of pyrazolo[3,4-*d*]-pyrimidine derivatives via miniaturized polymer−drug microarrays. *ACS Med. Chem. Lett.* **2018**, *9* (3), 193−197.
(40) Porter, A. G.; Jänicke, R. U. Emerging roles of caspase-3 in apoptosis. *Cell Death Differ.* **1999**, *6* (2), 99−104.
(41) Belmokhtar, C. A.; Hillion, J.; Ségal-Bendirdjian, E. Staurosporine induces apoptosis through both caspase-dependent and caspase-independent mechanisms. *Oncogene* **2001**, *20* (26), 3354−3362.
(42) Hoek, J. B.; Cahill, A.; Pastorino, J. G. Alcohol and Mitochondria: a dysfunctional relationship. *Gastroenterology* **2002**, *122* (7), 2049−2063.
(43) Rao, R. D.; Mladek, A. C.; Lamont, J. D.; Goble, J. M.; Erlichman, C.; James, C. D.; Sarkaria, J. N. Disruption of parallel and converging signaling pathways contributes to the synergistic antitumor effects of simultaneous mTOR and EGFR inhibition in GBM cells. *Neoplasia* **2005**, *7* (10), 921−929.
(44) Garuti, L.; Roberti, M.; Bottegoni, G. Multi-kinase inhibitors. *Curr. Med. Chem.* **2015**, *22* (6), 695−712.
(45) Chou, T.-C. Drug combination studies and their synergy quantification using the Chou-Talalay Method. *Cancer Res.* **2010**, *70* (2), 440−446.
(46) Yahiaoui, A.; Meadows, S. A.; Sorensen, R. A.; Cui, Z.-H.; Keegan, K. S.; Brockett, R.; Chen, G.; Quéva, C.; Li, L.; Tannheimer, S. L. PI3Kδ inhibitor idelalisib in combination with BTK inhibitor ONO/GS-4059 in diffuse large B cell lymphoma with acquired resistance to PI3Kδ and BTK inhibitors. *PLoS One* **2017**, *12* (2), No. e0171221.
(47) Taresco, V.; Louzao, I.; Scurr, D.; Booth, J.; Treacher, K.; McCabe, J.; Turpin, E.; Laughton, C. A.; Alexander, C.; Burley, J. C.; Garnett, M. C. Rapid nanogram scale screening method of microarrays to evaluate drug-polymer blends using high-throughput printing technology. *Mol. Pharmaceutics* **2017**, *14* (6), 2079−2087.
(48) Styliari, I. D.; Conte, C.; Pearce, A. K.; Hüsler, A.; Cavanagh, R. J.; Limo, M. J.; Gordhan, D.; Nieto-Orellana, A.; Suksiriworapong, J.; Couturaud, B.; Williams, P.; Hook, A. L.; Alexander, M. R.; Garnett, M. C.; Alexander, C.; Burley, J. C.; Taresco, V. High-throughput miniaturized screening of nanoparticle formation via inkjet printing. *Macromol. Mater. Eng.* **2018**, *303* (8), 1800146.
(49) Solassol, I.; Pinguet, F.; Quantin, X. FDA- and EMA-Approved tyrosine kinase inhibitors in advanced EGFR-mutated non-small cell lung cancer: safety, tolerability, plasma concentration monitoring, and management. *Biomolecules* **2019**, *9* (11), 668.
(50) Alonso-Gordoa, T.; García-Bermejo, M. L.; Grande, E.; Garrido, P.; Carrato, A.; Molina-Cerrillo, J. Targeting tyrosine kinases in renal cell carcinoma: ″new bullets against old guys″. *Int. J. Mol. Sci.* **2019**, *20* (8), 1901.
(51) Fallacara, A. L.; Zamperini, C.; Podolski-Renić, A.; Dinić, J.; Stanković, T.; Stepanović, M.; Mancini, A.; Rango, E.; Iovenitti, G.; Molinari, A.; Bugli, F.; Sanguinetti, M.; Torelli, R.; Martini, M.; Maccari, L.; Valoti, M.; Dreassi, E.; Botta, M.; Pešić, M.; Schenone, S. A New strategy for glioblastoma treatment: in vitro and in vivo preclinical characterization of Si306, a pyrazolo[3,4-*d*]pyrimidine dual Src/P-glycoprotein inhibitor. *Cancers* **2019**, *11* (6), 848.

https://dx.doi.org/10.1021/acsmedchemlett.9b00530
ACS Med. Chem. Lett. 2020, 11, 657−663

Development of Pyrazolo[3,4-*d*]pyrimidine Kinase Inhibitors as Potential Clinical Candidates for Glioblastoma Multiforme

Chiara Greco,† Vincenzo Taresco,‡ Amanda K. Pearce,§ Catherine E. Vasey,⊥ Stuart Smith,¶ Ruman Rahman,¶ Cameron Alexander,⊥ Robert J. Cavanagh,⊥,* Francesca Musumeci,†,* Silvia Schenone†

† Department of Pharmacy, University of Genoa, Viale Benedetto XV 3, 16132 Genoa, Italy

‡ School of Chemistry, University of Nottingham, University Park, Nottingham NG7 2RD, UK

§ School of Chemistry, University of Birmingham, Edgbaston, Birmingham B15 2TT, U.K

⊥School of Pharmacy, University of Nottingham, University Park, Nottingham NG7 2RD, U.K.

¶ Children's Brain Tumour Research Centre, School of Medicine, University of Nottingham, Nottingham NG7 2UH, UK

Table of contents

Chemicals

Polyvinylpyrrolidone-vinyl acetate copolymer (PVPVA), Tween 80, Pluronic F-68 and dimethyl sulfoxide (DMSO) were purchased from SIGMA Aldrich and the latter used as a common solvent to dissolve all the printable materials. Synthesis of pyrazolo[3,4-*d*]pyrimidines kinase inhibitors were performed by Prof. Schenone's group at the University of Genoa.[1,2,3]

Printing

Prior to dispensing the drug solution into a 96-well plate, the target had to be programmatically defined. The probe substrate consists of the well plate, drug solutions were dispensed via a piezoelectric inkjet printer (Sciflexarray S5, Scienion) using a 90 µm orifice nozzle. The droplet size was controlled by the values of the voltage and electrical pulse. A fixed amount of drug (20 µg) was dispensed for each well, by adjusting the number of drops. The number of drops per spot were selected in such way that the volume aspired delivered by the nozzle (max 10 µL) at the

beginning of a run was sufficient to print the whole print pattern. In a routine experiment DMSO solution (10 mg/mL) droplets with nominal volumes ranging from 250-280 pL, were dispensed at a 300 Hz jetting frequency by adjusting the voltage and pulse between 98-105 Volt (Voltage) and 45-55 μs (Pulse) respectively. The nozzle was washed with DMF, in between each printing cycle, as part of the automated printing-washing loop. DMSO was chosen due to both its high evaporation point that avoids nozzle blockage and its ability to dissolve all the selected drugs. SI306 and polymer solutions were prepared by dissolving the desired amount of compound in DMSO and, separately, the polymers in deionized (DI) water, in order to reach a final concentration of 5 μg/mL and 45 μg/mL, respectively.

Dynamic Light Scattering (DLS)

Dynamic Light Scattering (DLS) measurements were conducted in triplicate using a Malvern Zetasizer Nano ZS at 25^{o}C (scattering angle 173^{o}, laser of 633 nm) or a Viscotek 802 DLS with a laser wavelength of 830 nm at 20 ^{o}C. Formulations were prepared as above at 5 μg/mL (with respect to drug) in PBS. Data was analyzed using OmniSIZE software. A minimum of 10 measurements were collected per sample.

As can be observed from Figure 6 of the manuscript, all the formulations produced well-defined nanoaggregates, characterised by a single monomodal and monodispersed population with sizes ranging from 180 to 200 nm. The absence of a second peak or species related to aggregation confirmed the quality of the nanoformulation obtained due to the interactions between the small molecules and the different polymers. The amphiphilic nature of the macromolecules facilitated the interactions with the hydrophobic active compounds leading to an improvement of the self-assembly properties.

UV screening

Different commercial polymers (PEG8000, PEG20000, Pluronic F-68, Tween 80, PVPVA) were combined with SI306 (at a “drug”/polymer ratio of 10/90% w/w) and the apparent-solubility (ΔA%) value of each formulation was calculated in order to identify the polymers able to solubilise our lead compound. UV-vis spectra of SI306, commercial polymers and SI306-polymer formulations are reported in Figures 1SI and 2SI. Samples were diluted until the final concentration of 100 μg/mL and 900 μg/mL for SI306 and the polymers, respectively.

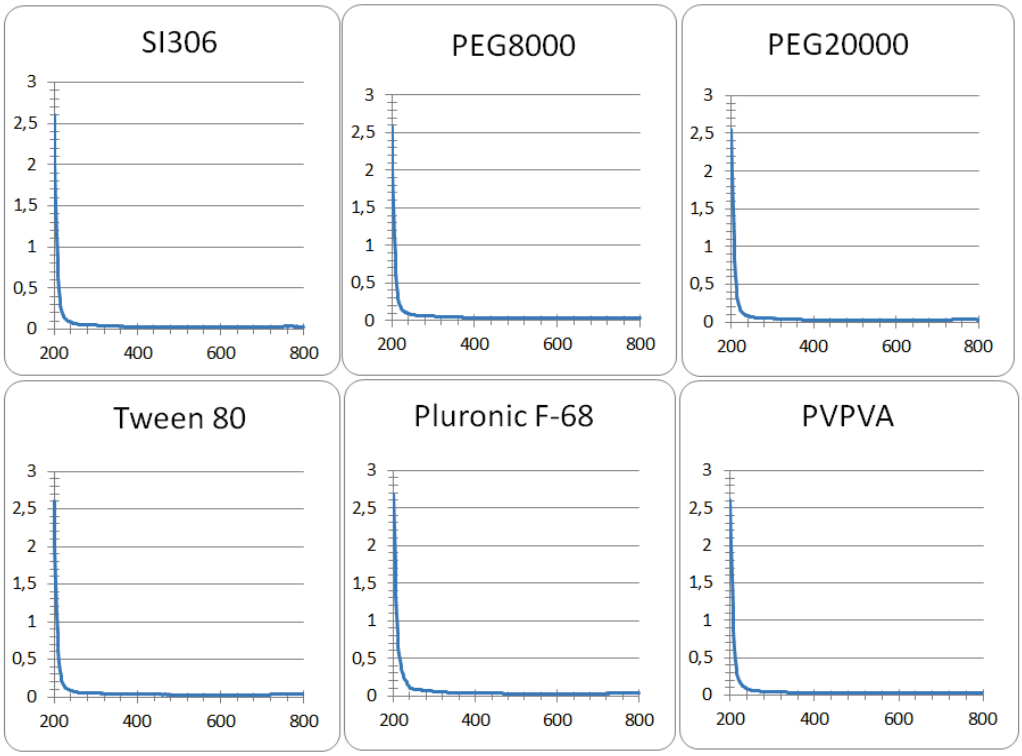

Figure 1SI. UV-vis spectra of SI306 (concentration 100 µg/mL) and selected commercial polymers (concentration 900 µg/mL) in PBS. We already demonstrated that solutions of in-house pyrazolo[3,4-*d*]pyrimidines in DMSO absorb in the UV region.[4]

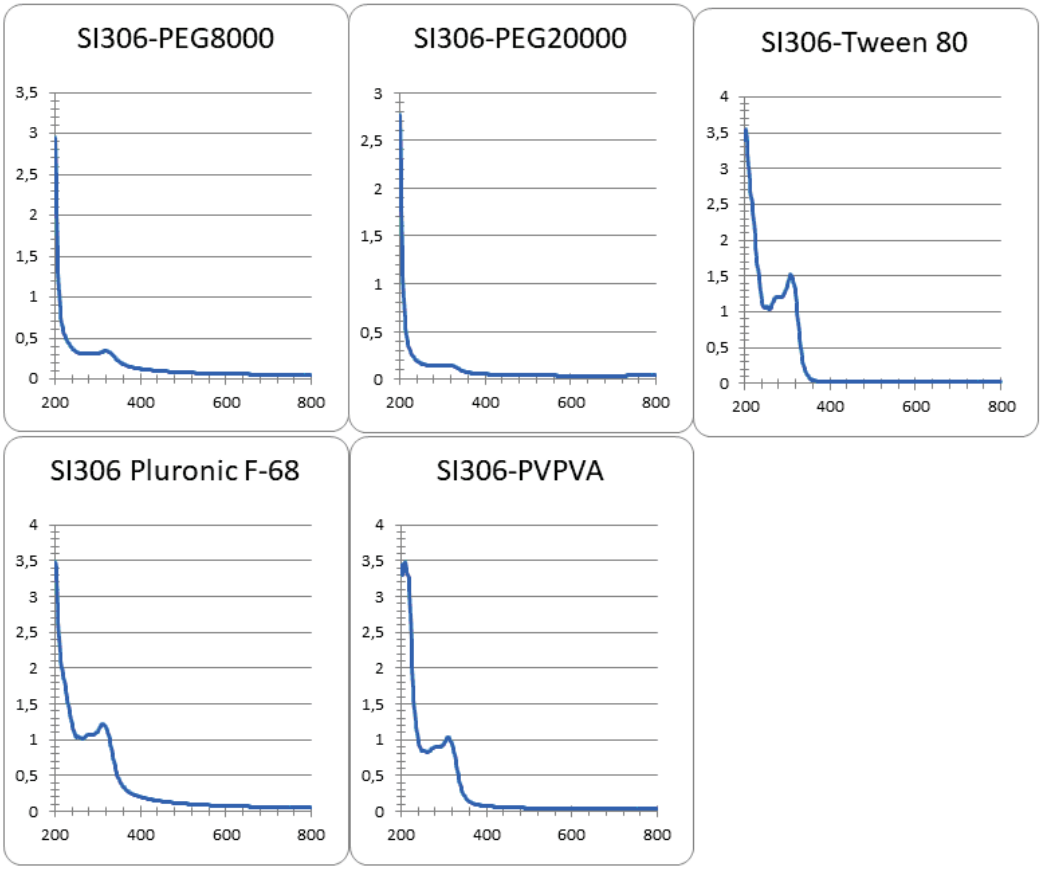

Figure 2SI. UV-vis spectra of SI306-polymer formulations in PBS (100 µg/mL of SI306 and 900 µg/mL of polymer).

ΔA% determination

ΔA% was calculated according the following equation:[4]

$$\Delta A\% = \frac{A - A_0}{A_0} \cdot 100$$

Where:
A_0 is the absorbance of the polymer solutions in water (used as blank),
A is the absorbance of the aqueous solutions of drug/polymer blends.
No signal was observed from the presence of water-insoluble SI306 (Figure 1SI).

In Table 1SI the ΔA% is reported for every SI306-polymer formulation.

Table 1SI. ΔA% of SI306 and polymers. Absorbance has been measured at λ = 308 nm

	PEG8000	**PEG20000**	**Tween80**	**Pluronic F68**	**PVPVA**
ΔA%	584.5179	555.3168	4251.295	2857.245	2312.342

Cell lines

GIN-8 (Glioma INvasive margin cells) isolated from medial front invasive margin (54F Wild type IDH (primary GBM), intact ATRX, 0% MGMT promoter methylation, 90% resection plus Gliadel wafers; Treatment 60Gy radiotherapy, concurrent and adjuvant temozolomide; patient died 5months after surgery), GIN-28 isolated from 5-ALA fluorescene invasive margin (71M Wild type IDH (primary GBM), intact ATRX, 0% MGMT promoter methylation 99% resection; no adjuvant therapy (patient choice); died 3 months after surgery) and GCE-28 (Glioma Contrast Enhanced core cells) isolated from central enhanced core region (same patient as GIN28) by Dr. Smith Dr. Rahman, and were used at passages of 15-30. Single tandem repeat (STR) genotyping is detailed in the **Figure 3SI.** The samples were paraffin-embedded and sectioned by the Queen's Medical Centre Histopathology Department. Cell lines were cultured in Dulbecco's Modified Eagle Medium (DMEM; Sigma-Aldrich) supplemented with 10% HyClone™ Bovine Growth Serum (BGS; GE Healthcare), 1g/L Glucose and 2 mM L-glutamine (Sigma-Aldrich) at 37°C with 5% CO_2.

DNA-System	DNA-criteria GIN-8 p11 CL181019_012	DNA-criteria GIN-8 p33 CL181019_013	DNA-criteria T8.3 CL181019_014	DNA-criteria GIN-28 p11 CL181019_021	DNA-criteria GIN-28 p33 CL181019_022	DNA-criteria GCE-28 p16 CL181019_023	DNA-criteria GCE-28 p19 CL181019_024	DNA-criteria T28.3 CL181019_025
AM	X, X	X, X	X, X	X, Y	X, Y	X, Y	X, Y	X, Y
D3S1358	15, 16	15, 16	15, 16	14, 17	14, 17	14, 17	14, 17	14, 17
D1S1656	12, 16	12, 16	12, 16	12, 16	12, 16	12, 16	12, 16	12, 16
D6S1043	14, 18	14, 18	14, 18	11, 13	11, 13	11, 13	11, 13	11, 13
D13S317	12, 12	12, 12	11, 12	11, 12	11, 12	11, 12	11, 12	11, 12
Penta E	6, 9	6, 9	6, 9	7, 17	7, 17	7, 17	7, 17	7, 17
D16S539	12, 12	12, 12	12, 12	9, 12	9, 12	9, 12	9, 12	9, 12
D18S51	16, 17	16, 17	16, 17	14, 17	14, 17	14, 17	14, 17	14, 17
D2S1338	17, 19	17, 19	17, 19	19, 23	19, 23	19, 23	19, 23	19, 23
CSF1PO	11, 11	11, 11	11, 11	11, 13	11, 13	11, 13	11, 13	11, 13
Penta D	12, 13	12, 13	12, 13	12, 14	12, 14	12, 14	12, 14	12, 13, 14
TH01	9, 9	9, 9	7, 9	6, 9.3	6, 9.3	6, 9.3	6, 9.3	6, 9.3
vWA	17, ?	17, 17	17, 17	14, 15	14, 15	14, 15	14, 15	14, 15
D21S11	30, 30	30, 30	30, 30	27, 33	27, 33	27, 33	27, 33	27, 33
D7S820	9, 10	9, 10	9, 10	8, 10	8, 10	8, 10	8, 10	8, 10
D5S818	12, 13	12, 13	12, 13	11, 12	11, 12	11, 12	11, 12	11, 12
TPOX	8, 11	8, 11	8, 11	8, 11	8, 11	8, 11	8, 11	8, 11
D8S1179	10, 13	10, 13	10, 13	10, 14	10, 14	10, 14	10, 14	10, 14
D12S391	18, 18	18, 18	18, 18	20, 21	20, 21	20, 21	20, 21	20, 21
D19S433	13, 13	13, 13	13, 13	14, 14	14, 14	14, 14	14, 14	13, 14
FGA	21, 22	21, 22	21, 22	23, 25	23, 25	23, 25	23, 25	23, 25

Figure 3SI: Single tandem repeat genotyping of patient-derived GBM cell lines. Cell line authentication of the GIN-8, GIN-28, and GCE-28 patient-derived primary lines isolated from the GBM invasive edge. DNA was isolated from each sample and genetic characteristics determined by PCR-single-locus-technology, utilizing 21 independent PCR-systems. The GIN-8 line compared across two passages (p11 and p33), showed identical STR genotypes, which fully matched the STR genotype from primary invasive margin GBM tissue (T8.3) from which the cells were derived. The GIN-28 line compared across two passages (p11 and p33), showed identical STR genotypes, with 20/21 DNA systems matching the STR genotype from primary invasive margin GBM tissue (T28.3) from which the cells were derived. Similarly, the GCE-28 line compared across two passages (p16 and p19), showed identical STR genotypes, with 20/21 DNA systems matching the STR genotype from primary GBM tissue (T28.3) from which the cells were derived. Note that GIN-28 and GCE-28 are invasive margin and contrast enhanced cell lines derived from the same patient. Collectively these results confirm that the cell lines utilised in this study have not been cross-contaminated with any other cell line and the primary lines derived from the GBM invasive margin broadly retain the genotype of the tumour.

Metabolic Activity.

Cells were seeded at a density of 1 x 10^4 cells per well in 96 well plates (Corning) for 24 hours prior to assaying. Dosing of cells was initiated by removing culture medium, washing cells with phosphate buffered saline (PBS; Sigma-Aldrich) and the application of 100 µL per well of treatment for 48 hours. Treatments were applied to cells in phenol red free DMEM (Thermo-Fisher) containing 10% BGS. Pyrazolo[3,4-*d*]pyrimidine-based kinase inhibitors were dosed at concentrations of 0.78 – 50.00 µg/mL for determination of their half maximal inhibitor concentration (IC_{50}) values, and at 5 µg/mL for evaluation of their activity in formulations. Additionally, to study the cytocompatibility of the DMSO concentration used to dissolve free drugs, medium containing 1% (v/v) DMSO was applied to cells. Cells were also treated with 0.1% (v/v) Triton-X 100 and DMEM with 10% BGS for 48 h for use as positive and negative controls, respectively. Following treatment, cells were washed with PBS and incubated with 100 µl 10% PrestoBlue™ Cell Viability Reagent diluted in medium per well for 1 h. Solution fluorescence was then measured at 560/600 nm (λex/λem), and relative metabolic activity calculated by setting the values of the negative control as 100% and the positive control (0.1% Triton X-100) as 0%. The metabolic viability graphs are reported in **Figure 4SI**.

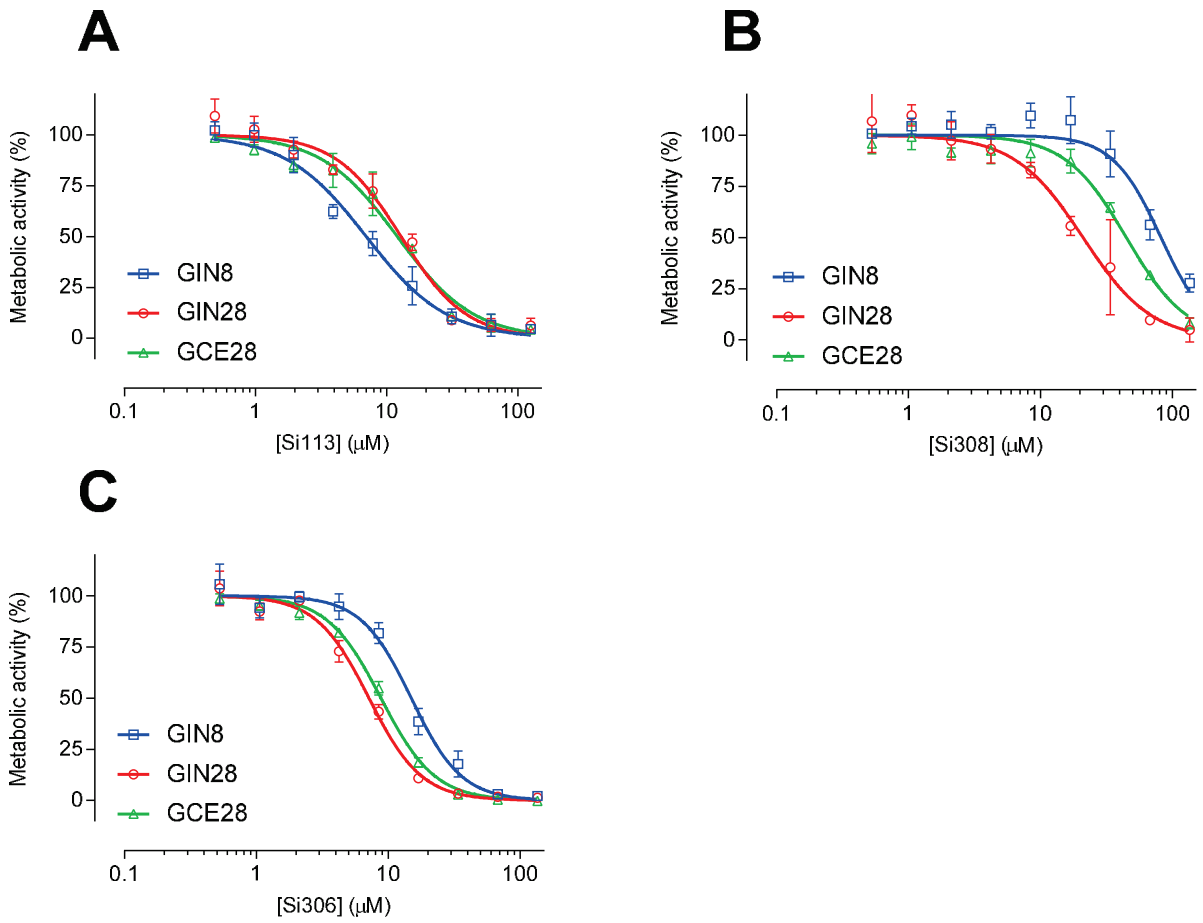

Figure 4SI. Effect of of (A) SI113, (B) SI308 and (C) SI306 compounds on cellular metabolic activity as determined by the PrestoBlue assay. Compounds were applied diluted in 10% FBS containing DMEM for 48h. Data are presented as mean ± SD (n=3).

In the **Figure 7** of the manuscript, compound SI306 formulated with the selected best polymers was tested against the patients derived GBM cell lines and the potency compared to the compound solubilized in 1% DMSO. The formulated compounds were diluted reaching a concentration of 5 µg/mL and 45 µg/mL for SI306 and the polymers, respectively ("drug"/polymer ratio of 10/90% w/w), using 10% FBS containing DMEM.

Detection of Activated Caspase-3/7.

The CellEvent caspase-3/7 green detection reagent (Thermo Fisher Scientific) was employed to evaluate levels of activated caspase-3 or -7. After exposure to the drugs solutions, 150 µL of 2% (v/v) CellEvent probe in PBS was applied per well for 30 min at 37 °C. Staurosporine was used at 10 µM as the apoptotic control. Fluorescent intensity was measured at 502/530 nm (λex/λem) and normalized to the untreated control (set as a value of 1).

Hoechst 33342/Propidium Iodide Microscopy.

Integrity of the nuclear membrane and nuclear fragmentation was measured by propidium iodide (PI; Thermo Fisher Scientific) uptake. To do so, 6 × 10^4 GIN28 and GCE28 cells per well were seeded in 24-well plates (Corning) and cultured for 24h. Following this, treatment solutions, including selected kinase inhibitors, or 100% ice cold ethanol were applied for 48h.
Treatments were then aspirated, and the cells were washed with PBS, followed by the addition of 1 µM Hoechst 33342 (Thermo Fisher Scientific) in PBS for 5 min and then 0.1 mg/mL of PI in PBS (final concentration ~2 µg/mL PI). The cells were incubated for another 5 min, after which the solution was removed, and the cells were washed with PBS. Cells were then imaged on an inverted Nikon Eclipse TE 300 microscope using a DAPI filter (357/447 nm; excitation/emission) for detection of the Hoechst signal and the RFP filter (531/593 nm; excitation/emission) for the PI signal.

Statistical analysis.

Dose-response curve fitting was performed using non-linear regression analysis to enable IC_{50} determination (GraphPad prism, version 7.03). Statistical analysis was performed by one-way ANOVA with Dunnett's multiple comparison post hoc test using GraphPad prism.

Determination of Combination Index (CI) values

CI values were determined according to a widely used method established by Chou and Talalay.[5,6] Briefly, in order to determine each CI value, the following cytotoxicity studied were conducted: (1) SI113 as a single compound, (2) SI308 as a single compound, (3) SI306 as a single compound, (4) S306 + SI308 combination, (5) SI113 + SI308 combination and (6) SI113 + SI306 combination. Compounds were applied in combination at a molar ratio of 1:1, and dosed with a range of 0.1 – 100.0 µM per compound. IC_{50} values were then calculated from each study and used in the following equation to determine CI values;

$$\mathbf{CI} = \frac{\mathbf{D_{CA}}}{\mathbf{D_{SA}}} + \frac{\mathbf{D_{CB}}}{\mathbf{D_{SB}}} + \frac{\mathbf{D_{CA}}\,\mathbf{D_{CB}}}{\mathbf{D_{SA}}\,\mathbf{D_{SB}}}$$

Where D_{CA} represents the IC_{50} values of drug A in combination with drug B, and D_{SA} the IC_{50} of drug A as a single compound. Similarly, D_{CB} represents the IC_{50} values of drug B in combination with drug A, and D_{SB} the IC_{50} of drug B as a single compound. Based on this method, CI values are indicative of strong synergism (<0.7), synergism (0.7-0.9), additive effect (0.9-1.1), antagonism (1.1-3.3), or strong antagonism (>3.3).[5] Microsoft Excel was then employed to produce a tricolor system based on these values, where antagonism is represented by red, additive effect by yellow, and synergism by green.

References

(1) Tintori, C.; Fallacara, A. L.; Radi, M.; Zamperini, C.; Dreassi, E.; Crespan, E.; Maga, G.; Schenone, S.; Musumeci, F.; Brullo, C.; Richters, A.; Gasparrini, F.; Angelucci, A.; Festuccia,

C.; Delle Monache, S.; Rauh, D.; Botta, M.Combining X-ray crystallography and molecular modeling toward the optimization of pyrazolo[3,4-*d*]pyrimidines as potent c-Src inhibitors active in vivo against neuroblastoma. *J. Med. Chem.* **2015**, *58* (1), 347–361.

(2) Tintori, C.; La Sala, G.; Vignaroli, G.; Botta, L.; Fallacara, A. L.; Falchi, F.; Radi, M.; Zamperini, C.; Dreassi, E.; Dello Iacono, L.; Orioli, D.; Biamonti, G.; Garbelli, M.; Lossani, A.; Gasparrini, F.; Tuccinardi, T.; Laurenzana, I.; Angelucci, A.; Maga, G.; Schenone, S.; Brullo, C.; Musumeci, F.; Desogus, A.; Crespan, E.; Botta, M. Studies on the ATP binding site of Fyn kinase for the identification of new inhibitors and their evaluation as potential agents against tauopathies and tumors. *J. Med. Chem.* **2015**, *58* (11), 4590–4609.

(3) Radi, M.; Dreassi, E.; Brullo, C.; Crespan, E.; Tintori, C.; Bernardo, V.; Valoti, M.; Zamperini, C.; Daigl, H.; Musumeci, F.; Carraro, F.; Naldini, A.; Filippi, I.; Maga, G.; Schenone, S.; Botta, M. Design, Synthesis, biological activity, and ADME properties of pyrazolo[3,4- *d*]pyrimidines active in hypoxic human leukemia cells: a lead optimization study. *J. Med. Chem.* **2011**, *54* (8), 2610–2626.

(4) Sanna, M.; Sicilia, G.; Alazzo, A.; Singh, N.; Musumeci, F.; Schenone, S.; Spriggs, K. A.; Burley, J. C.; Garnett, M. C.; Taresco, V.; Alexander, C. Water solubility enhancement of pyrazolo[3,4- *d*]pyrimidine derivatives via miniaturized polymer–drug microarrays. *ACS Med. Chem. Lett.* **2018**, *9* (3), 193–197. h

(5) Chou, T.-C. Theoretical Basis, experimental design, and computerized simulation of synergism and antagonism in drug combination studies. *Pharmacol. Rev.* **2006**, *58* (3), 621–681.

(6) Chou, T.-C. Drug Combination studies and their synergy quantification using the Chou-Talalay Method. *Cancer Res.* **2010**, *70* (2), 440–446.